SCIENTIFIC REPORTS

OPEN

SUBJECT AREAS:
CELL GROWTH
REGENERATION

Received
11 December 2013

Accepted
12 June 2014

Published
3 July 2014

Correspondence and requests for materials should be addressed to X.C. (chenxiao-610@zju.edu.cn) or H.W.O. (hwoy@zju.edu.cn)

Fetal and adult fibroblasts display intrinsic differences in tendon tissue engineering and regeneration

Qiao-Mei Tang[1,2], Jia Lin Chen[1,2], Wei Liang Shen[3], Zi Yin[1,2], Huan Huan Liu[1,2], Zhi Fang[1,2], Boon Chin Heng[4], Hong Wei Ouyang[1,2] & Xiao Chen[1,2]

[1]Department of Sports Medicine, School of Medicine, Zhejiang University, Hangzhou, China, 310058, [2]Zhejiang Provincial Key Laboratory of Tissue Engineering and Regenerative Medicine School of Medicine, Zhejiang University, Hangzhou China. 310058, [3]Department of Orthopedic Surgery, 2nd Affiliated Hospital, Zhejiang University, Hangzhou, China, 310058, [4]Department of Biosystems Science & Engineering (D-BSSE), ETH-Zurich, Mattenstrasse 26, Basel 4058, Switzerland.

Injured adult tendons do not exhibit optimal healing through a regenerative process, whereas fetal tendons can heal in a regenerative fashion without scar formation. Hence, we compared FFs (mouse fetal fibroblasts) and AFs (mouse adult fibroblasts) as seed cells for the fabrication of scaffold-free engineered tendons. Our results demonstrated that FFs had more potential for tendon tissue engineering, as shown by higher levels of tendon-related gene expression. In the *in situ* AT injury model, the FFs group also demonstrated much better structural and functional properties after healing, with higher levels of collagen deposition and better microstructure repair. Moreover, fetal fibroblasts could increase the recruitment of fibroblast-like cells and reduce the infiltration of inflammatory cells to the injury site during the regeneration process. Our results suggest that the underlying mechanisms of better regeneration with FFs should be elucidated and be used to enhance adult tendon healing. This may assist in the development of future strategies to treat tendon injuries.

Tendon injury occurs frequently during sports and other rigorous physical activities, and surgical intervention is required to reconstruct the shoulder's rotator cuff tendons (51,000 per year), the Achilles tendons (44,000 per year), and the patellar tendons (42,000 per year)[1]. Autografts, allografts and xenografts have various drawbacks such as donor site morbidity[2,3], immunological rejection[4], and poor graft integration[5]. However, due to poor healing capacity of native tendons, tissue regeneration after injury remains a formidable challenge. It is well known that tendons do not heal by a regenerative process. Instead, tendon healing is often accompanied by the formation of a fibrotic scar which impairs mechanical strength of the tissue, and some tendon injuries do result in significant dysfunction and disability[6–8]. Obviously, better alternative treatment modalities need to be developed.

Cell therapy and tissue engineering have made great strides during the last decade, and have demonstrated much potential for application in tendon repair and regeneration[9–16]. Appropriate seed cells are absolutely crucial for successful tendon tissue engineering. Currently, commonly utilized seed cells in tendon tissue engineering include tenocytes, fibroblasts and mesenchymal stem cells. Because tendon progenitor/stem cells have to be isolated directly from tendon tissues, there is inevitable donor site morbidity, and hence it is not practical to utilize these cells for tendon repair due to secondary trauma to the donor site[17]. Mesenchymal stem cells (MSCs) are also potential seed cells for tendon reconstruction. However, it is difficult to control their differentiation into specific tissue lineages[18,19]. Considering the fact that both tenocytes and dermal fibroblasts are of mesodermal origin and that both these cell types exhibit similar spindle-shaped morphology during in vitro culture and produce major extracellular matrix proteins such as collagen; it is possible that dermal fibroblasts could be promising seed cells for in vivo tendon tissue engineering[20–22]. Moreover, dermal fibroblasts are an easily accessible cell source. Harvesting a small piece of skin tissue will not cause major donor site morbidity, which is advantageous for clinical repair[22,23]. Hence, dermal fibroblasts can serve as an appropriate seed cell for tendon tissue engineering.

However, previous studies have shown that adult tendons do not heal optimally through a regenerative process[24–26], and is usually accompanied by scar tissue formation. In contrast, although the biomechanical function of healed fetal tendon after injury is inferior to that of native fetal tendon[25], fetal tendons heal in a regenerative fashion without scar formation. More interestingly, the adult environment is in fact not a barrier to scar-free tendon repair and that this healing capacity is intrinsic to the fetal tendon itself[25]. There is substantial

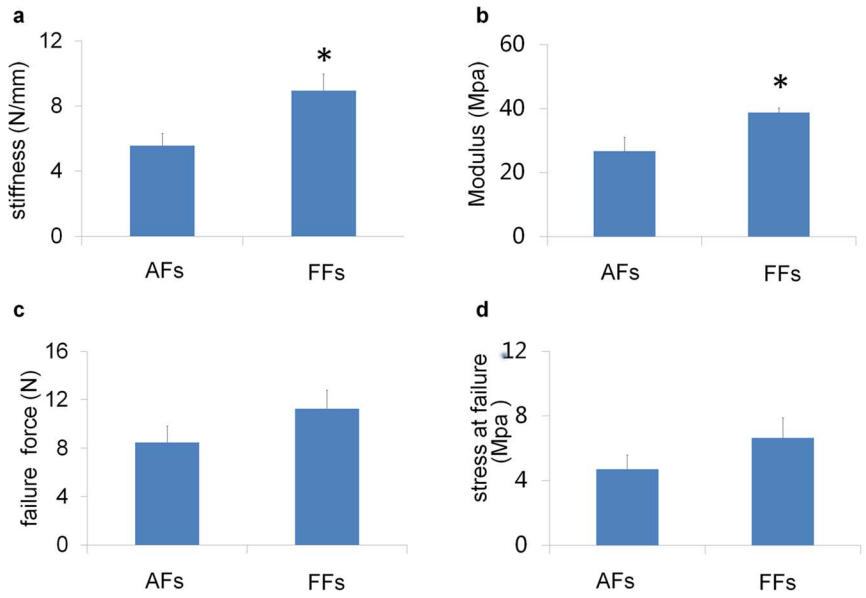

Figure 1 | Mechanical properties of repaired tendons at 4 weeks post-surgery. Samples were carefully attached for mechanical testing on the Instron machine. The stiffness (a), modulus (b), failure force (c) and stress at failure (d) of the FFs repaired tendon were higher than the AFs repaired tendon $p < 0.05$. ** $P < 0.01$ between two groups. Abbreviations: mouse fetal fibroblasts (FFs) and mouse adult fibroblasts (AFs).

evidence that early and mid-gestational fetal tissues respond to injury in a radically different way compared to adult tissues. A scar-free healing response has been observed in nerve, uterus, and bone injury models[27–29]. Similarly, this phenomenon can also be observed with fetal skin repair[30,31]. However, the underlying mechanism of scar-free fetal repair remains unclear. The extracellular matrix, cytokines and inflammatory responses of fetal and adult wounds exhibit significant differences[32–34]. There is evidence that the recruitment of inflammatory cells to the wound site may play a role in scar formation[35]. Other studies suggest that the differences between fetal and adult skin wound healing are intrinsic to fetal fibroblasts[30,36,37]. Indeed, isolated human fetal skin transplanted into adult athymic mice can heal without scarring[38]. Therefore, fetal cells may be more appropriate seed cells for improved tissue engineering.

We hereby hypothesize that fetal cells are better suited for tendon tissue engineering compared to adult cells. In this study we compared FFs (fetal fibroblasts) and AFs (adult fibroblasts) as seed cells for the fabrication of scaffold-free engineered tendons. These will be characterized *in vitro*, as well as evaluated *in vivo* within a mice Achilles Tendon (AT) injury model. The results demonstrated that utilizing FFs instead of AFs led to enhanced tendon regeneration, resulting in a more physiological structure and better biomechanical properties.

Results

Better mechanical properties of FFs-repaired tendons compared to AFs-repaired tendons. The mechanical properties of the repaired tendons were evaluated using an Instron tension system. Harvested specimens ($n = 5$ for the FFs group, $n = 7$ for the AFs group) were subjected to tests of maximal load, stiffness, emerge and stress at failure with the Instron mechanical testing machine (Fig. 1a–d). The results showed that FFs-repaired tendons had better mechanical properties than AFs-repaired tendons. The cross-sectional areas of the FFs and AFs-repaired tendons were 1.8 ± 0.4 mm^2 and 2.2 ± 1.5 mm^2 respectively. The stiffness in the FFs-repaired group was significantly higher than the AFs-repaired group (9.0 ± 1.0 vs. 5.6 ± 0.8 N/mm; $p < 0.05$). The stiffness measured for the FFs-repaired and AFs-repaired groups were 65.2% and 40.5% of that of the sham procedure group tendon respectively (13.7 ± 1.1 N/mm, $p < 0.01$). The modulus of the FFs-repaired tendons was 45% higher than that of the AFs-repaired tendons (38.8 ± 1.4 vs. 26.7 ± 4.4 MPa; $p < 0.05$). These values were 32.0% and 22.0% of that of the sham procedure group tendon (121.3 ± 12.1 MPa, $p < 0.01$). The maximum force of FFs-repaired tendons was 31.8% higher than that of the AFs-repaired group (11.2 ± 1.5 vs. 8.5 ± 1.3 N). The stress at failure of the tendons from the FFs-repaired group was slightly higher than that of the AFs-repaired group (6.6 ± 1.2 vs. 4.7 ± 0.9 Mpa; $p > 0.05$).

FFs engineered tendon has higher expression levels of tendon-related genes and displayed more ECM deposition *in vitro*. Both the FFs and AFs displayed spindle-shaped morphology (Fig. 2a and b). FFs proliferate more rapidly compared to AFs on day 1, 3, 5 and 7 (Fig. 2c). The expression levels of tendon-related genes, including Collagen type I (Col I), Collagen type III (Col III), Biglycan (Bgn), Nfatc 4 and Epha 4 were evaluated by QPCR during the process of forming the engineered tendon (Fig. 2d).The results demonstrated that the expression levels of tendon-related ECM (extracellular matrix) genes of FFs, including collagen III and BGN, were significantly higher at the early stage, as compared to that of AFs. The mRNA transcript levels of NFATC4 in FFs were consistently higher than AFs on day 0 (7.29-fold, $p < 0.01$) and 3 (1.43-fold, $p < 0.01$). The same trend was observed with EPHA4, with 3.23, 4.05, 2.43-fold higher expression levels in FFs compared to AFs on day 0, 3, & 7 respectively. The higher expression levels of tendon-related genes may contribute to better repair capacity of FFs in tendon injuries. The engineered tendon was formed after culturing the cell sheet for 14 days. FFs engineered tendon produced more extracellular matrix than AFs (Fig. 2e). Masson trichrome staining showed that more collagen fibers were formed in the FFs engineered tendon.

Gross morphology and cell survival over 4 weeks. After 4 weeks post-implantation of the engineered tendon within the mouse AT injury model, the gross morphology of the repaired tendons was observed. The regenerated tissue, both in the FFs and AFs group, integrated well with the surrounding normal tissues. The survival of the implanted cells at the injury site was monitored using a non-invasive CCCD tracking system and fluorescence microscopy. Image tracking showed that most of the implanted cells were distributed at the wound site at 2 and 4 weeks[39]. The survival of cells within the AFs-group and FFs-group at 2 weeks were similar (Fig. 3b and c).

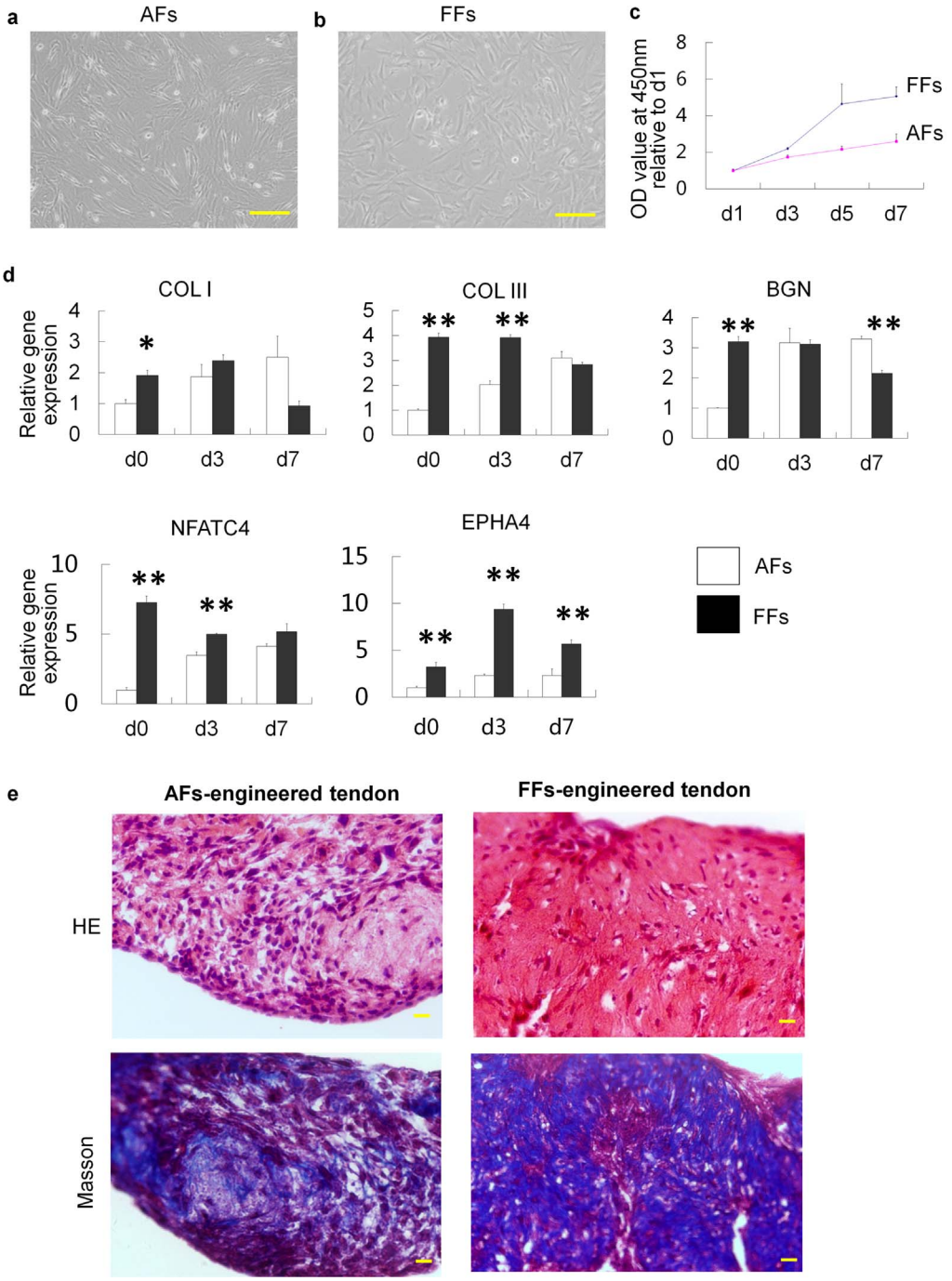

Figure 2 | ***In vitro*** **construction and characterization of scaffold-free engineered tendon.** (a–b) Morphology of mouse fetal fibroblasts (FFs) and mouse adult fibroblasts (AFs). (c): Cell proliferation of FFs and AFs on day 1, 3, 5, 7 showed high proliferation potential of FFs. (d): quantitative real time PCR confirmed gene expression levels of tendon-related genes expressed by FFs and AFs on day 0, 3, 7 of scaffold-free engineered tendon formation (n = 3, means ± SD). Gene expression levels are normalized to the reference gene GAPDH (y axis); Transcript levels expressed relative to day 0 AF samples. FFs engineered tendon showed high expression of tendon-related genes. * $P < 0.05$ between two groups. ** $P < 0.01$ between two groups. (e): Hematoxylin and eosin and Masson-stained sections of *in vitro* engineered tendons showing bands of collagen fibers. More collagen fibers were formed in the FFs engineered tendon. Scale bar = 200 μm (a) and (b); Scale bar = 20 μm (e).

This was confirmed by an in situ fluorescence study performed on the surgically treated tendon samples (Fig. 3d–j). The cell survival ratio were similar between the two groups and the survival ratio of both groups were reduced at 4 weeks post-surgery (0.91 ± 0.08 vs. 0.76 ± 0.13 at 2 weeks post-surgery, 0.48 ± 0.08 vs. 0.41 ± 0.05 at 4 weeks post-surgery, Fig. 3k–q, $P > 0.05$). Under fluorescence microscopy, we found that the labeled cells contributed to the injury site as tendon-like cells, characterized by a spindle shape, and oriented along the direction of mechanical force (Fig. 3d–q). These results indicated that the FFs and AFs were still alive and contribute to the injury site after 2 and 4 weeks post-surgery.

Histology of repaired tendon. After 1 week post-surgery, the repair site was composed mostly of fibroblasts and inflammatory cells. Nevertheless, compared with the AFs group, the FFs group had greater number of cells exhibiting parallel alignment along the axis

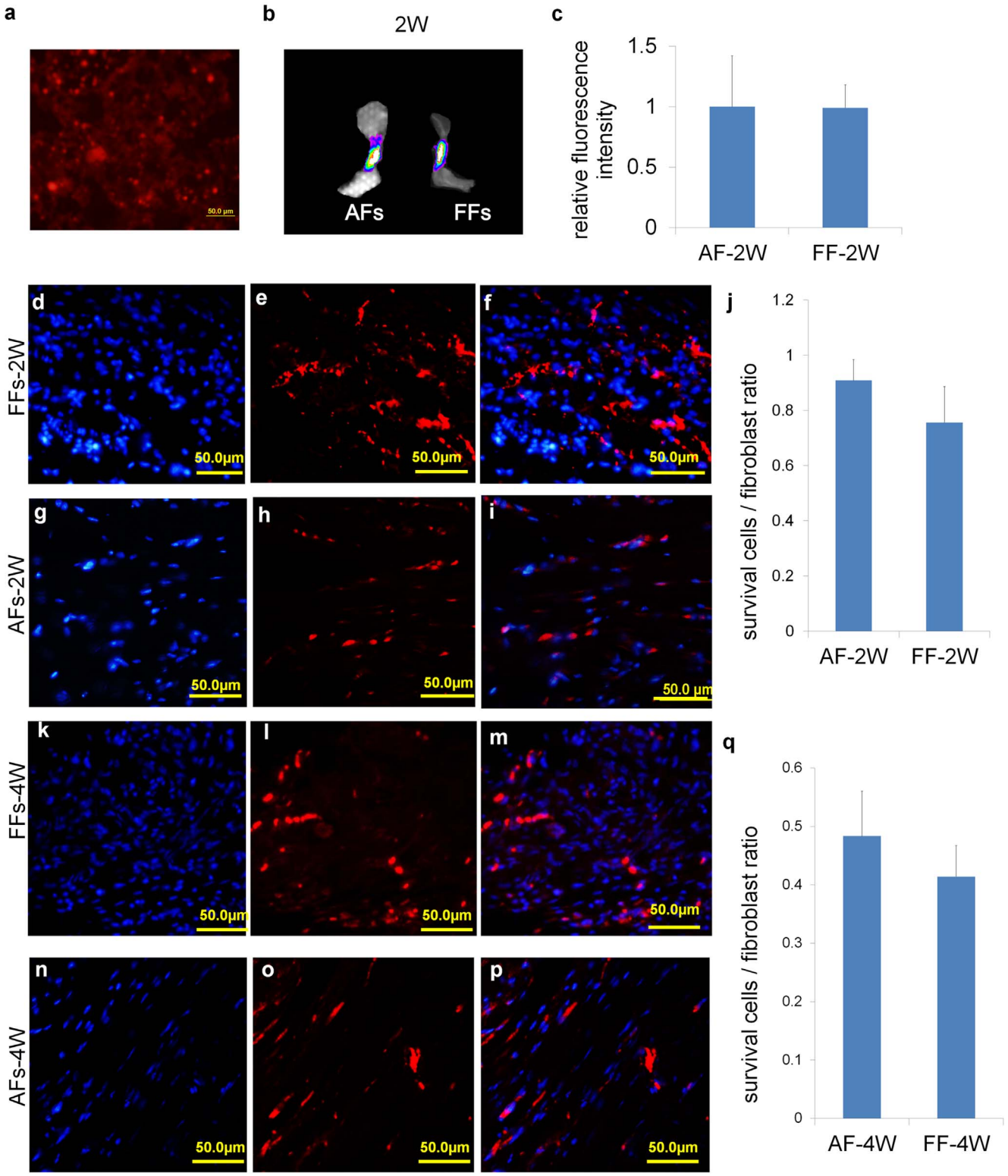

Figure 3 | FFs and AFs contributed to tendon repair. (a) DiI-stained cells were incorporated within engineered tendons. Then the cells were placed within the tendon defect and sutured to the tendon. (b): Fluorescence detection using a tracking system showed positive orange fluorescent signal existent in the implantation site, indicating positive cell survival after 2 weeks post-implantation. (c): The quantization of relative fluorescence intensity of AFs group and FFs group at 2 weeks post-transplantation. (e–j) and (i–q) denote the fluorescent staining results of the implanted constructs, showing that seed cells survived at the tendon defect and formed tendon-like tissues after 2 and 4 weeks post-surgery. (e), (h), (l) and (o) showed DAPI staining, (f), (i), (m) and (p) showed DiI staining, while (g), (j), (n) and (q) are the merged images of (e), (h), (l), (o) and (f), (i), (m), (p) respectively. (k), (r): The quantization of survived cells/fibroblast ratio of AFs group and FFs group at 2 and 4 weeks post-transplantation respectively. Abb: mouse fetal fibroblasts (FFs) and mouse adult fibroblasts (AFs).

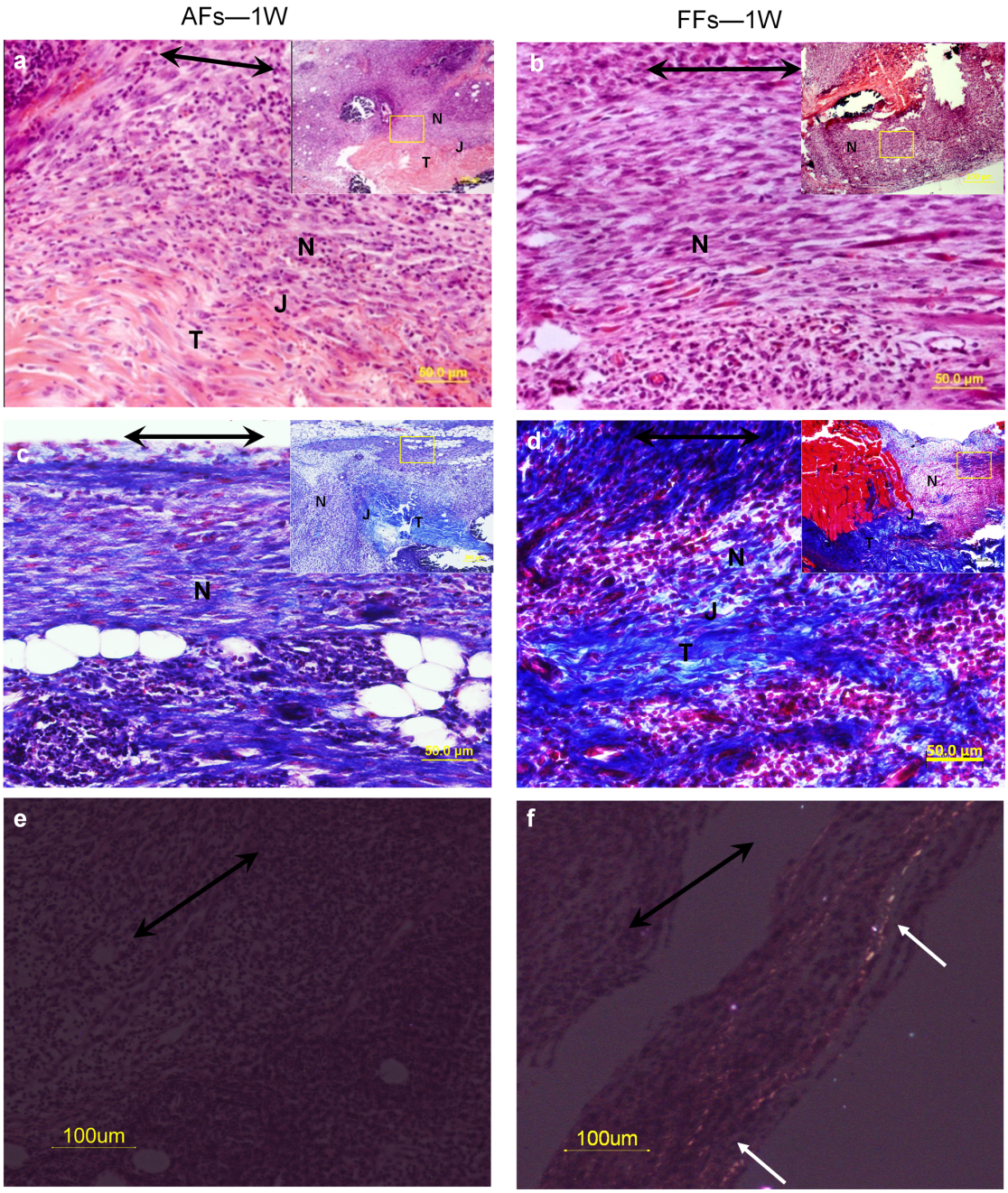

Figure 4 | Histology of scaffold-free engineered tendons after 1 week implantation in vivo. HE (a) and (b) and Masson trichrome (c) and (d) staining of tendon-like tissue showed tissue morphology and ECM deposition. The repaired site was composed mostly of fibroblast and inflammatory cells. Masson trichrome staining showed dense formation of collagen fibers at the repaired site. (e), (f) polarized light microscopy images of tissue-engineered tendon in vivo. The maturity of repaired tissues can be assessed under polarized light microscopy. Dark arrows indicate the axis of tensile load of the tendons. White arrow shows the collagen fibers under polarized light microscopy. Abbreviations: J - tendon-neotendon junction; N - neo-tendon; T - host tendon.

of tensile load and less inflammatory cells (Fig. 4a and b). Masson trichrome staining showed dense formation of collagen fibers at the repair site (Fig. 4c and d). Under polarized light microscopy, mature collagen fibrils were observed in the FFs-repaired group (Fig. 4e and f), but not in the AFs group. The histology score also showed that FFs-repaired tendons displayed more physiological histology than the AFs-repaired tendons (12.94 ± 1.18 vs. 14.42 ± 0.12). After two weeks post-implantation, HE staining showed a decrease in the number of infiltrating inflammatory cells in both the FFs-repaired and AFs-repaired groups[40] (Fig. 5a and b). Extracellular matrix with crimp pattern deposition and the existence of wavy parallel mature tendon-like cells were observed within the repaired tendons of the FFs group, whereas the repaired tendons of the AFs group exhibited looser, disarranged soft tissue (Fig. 5c and d). The maturity of the repaired tissue can be assessed under polarized light microscopy (Fig. 5e and f). The FFs-repaired group had a similar histology score compared to the AFs-repaired group (9.75 ± 1.80 vs. 10.96 ± 1.47).

After 4 weeks post-implantation, the FFs-repaired tendons showed denser ECM deposition, with more spindle-shaped cells compared with the AFs-repaired group (Fig. 6a and b). Additionally, a higher degree of cell alignment was also observed in the

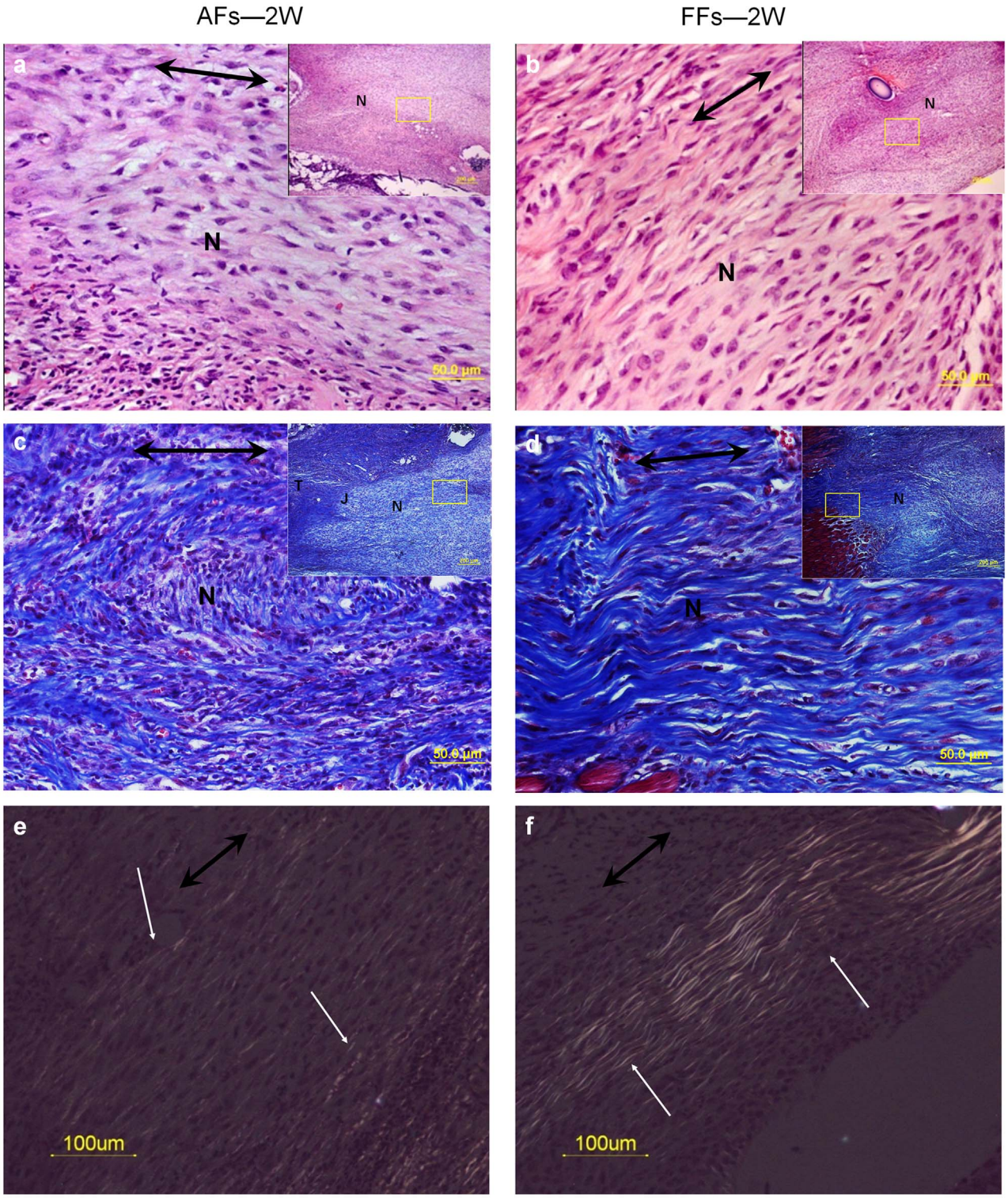

Figure 5 | Histology of scaffold-free engineered tendons after 2 weeks implantation *in vivo*. HE (a) and (b) and Masson trichrome (c) and (d) staining of tendon-like tissue showed tissue morphology and ECM deposition. HE staining showed a decrease in the number of inflammatory cell infiltration in both FFs-repaired and AFs-repaired groups. Masson trichrome staining indicated extracellular matrix with crimp pattern deposition in the FFs-repaired group. (e), (f) are polarized light microscopy images of tissue-engineered tendon *in vivo*. Dark arrows indicate the axis of tensile load of the tendons. White arrow shows the collagen fibers under polarized light microscopy. Abbreviations: J - tendon-neotendon junction; N - neo-tendon; T - host tendon.

FFs-repaired group. The neo-tendon exhibited arranged bundles of collagen fibers, which more closely resembled the native structure of tendon ECM (Fig. 6c and d). Under polarized light microscopy, continuous collagen fibers (bright yellow) were observed over the entire field of vision in the FFs-repaired tendons (Fig. 6f), unlike the AFs-repaired tendons (Fig. 6e). This indicated more mature collagen deposition in the FFs group, which correlated with the biomechanical data[41]. Although the histology score between the FFs-repaired

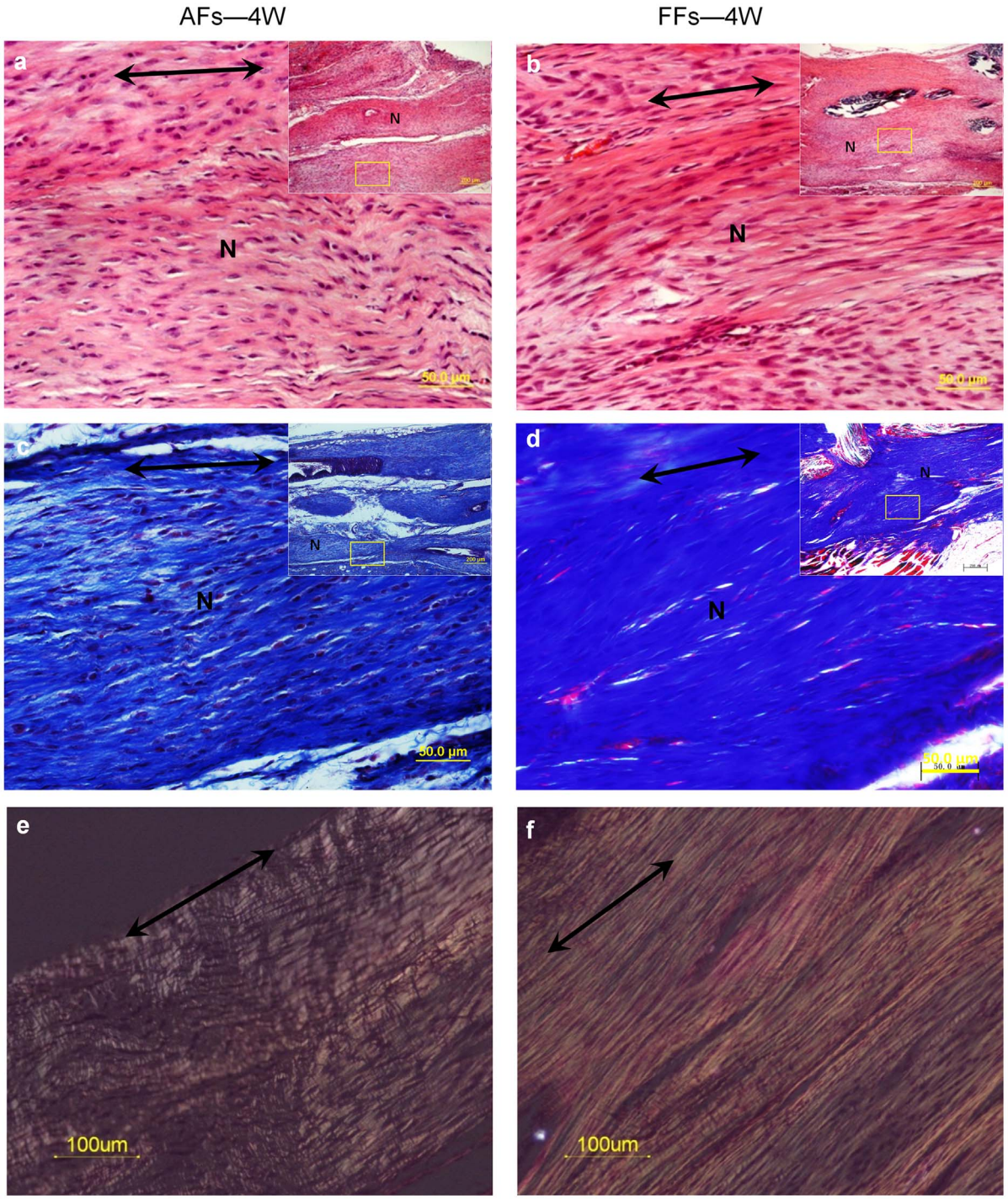

Figure 6 | Histology of scaffold-free engineered tendons after 4 weeks implantation *in vivo*. HE (a) and (b) and Masson trichrome (c) and (d) staining of tendon-like tissue showed tissue morphology and ECM deposition. The FFs-repaired tendons displayed more spindle-shaped cells and more arranged bundles of collagen fibers compared to the AFs-repaired group. (e), (f) are polarized light microscopy images of tissue-engineered tendon *in vivo*. Continuous collagen fibers (bright yellow) were observed over the entire field of vision in the FFs-repaired tendons. Dark arrows indicate the axis of tensile load of the tendons. White arrow shows the collagen fibers under polarized light microscopy. Abbreviations: N - neo-tendon.

group and AFs-repaired group were not significantly different, the FFs-repaired group showed an improvement compared to the AFs-repaired group (6.83 ± 2.68 vs. 8.63 ± 2.46). The lack of statistically significant difference may be due to the small sampling size.

Higher ratio of fibroblast-like cells and reduced number of immune cells within the FFs-repaired versus AFs-repaired tendons. After one week post-surgery, the FFs-repaired group was composed of 43 ± 7.2% fibroblast-like cells and 57 ± 7.2% immune cells, which differed significantly from the AFs-repaired group. The AFs-repaired group was composed of 23 ± 14.2% fibroblast-like cells and 77 ± 14.2% immune cells (Fig. 7a; $p < 0.05$). After two weeks, the FFs-repaired group was made up of 54 ± 11.0% fibroblast-like cells and 46 ± 11.0% immune cells, while the AFs-repaired group was composed of 34 ± 4.2% fibroblast-like cells and 66 ± 4.2% immune cells (Fig. 7b; $p < 0.05$). After 3 weeks post-surgery, the FFs-repaired group was composed of 56 ± 5.6% fibroblast-like cells and 44 ± 5.6% immune cells, whereas in the AFs-repaired group the

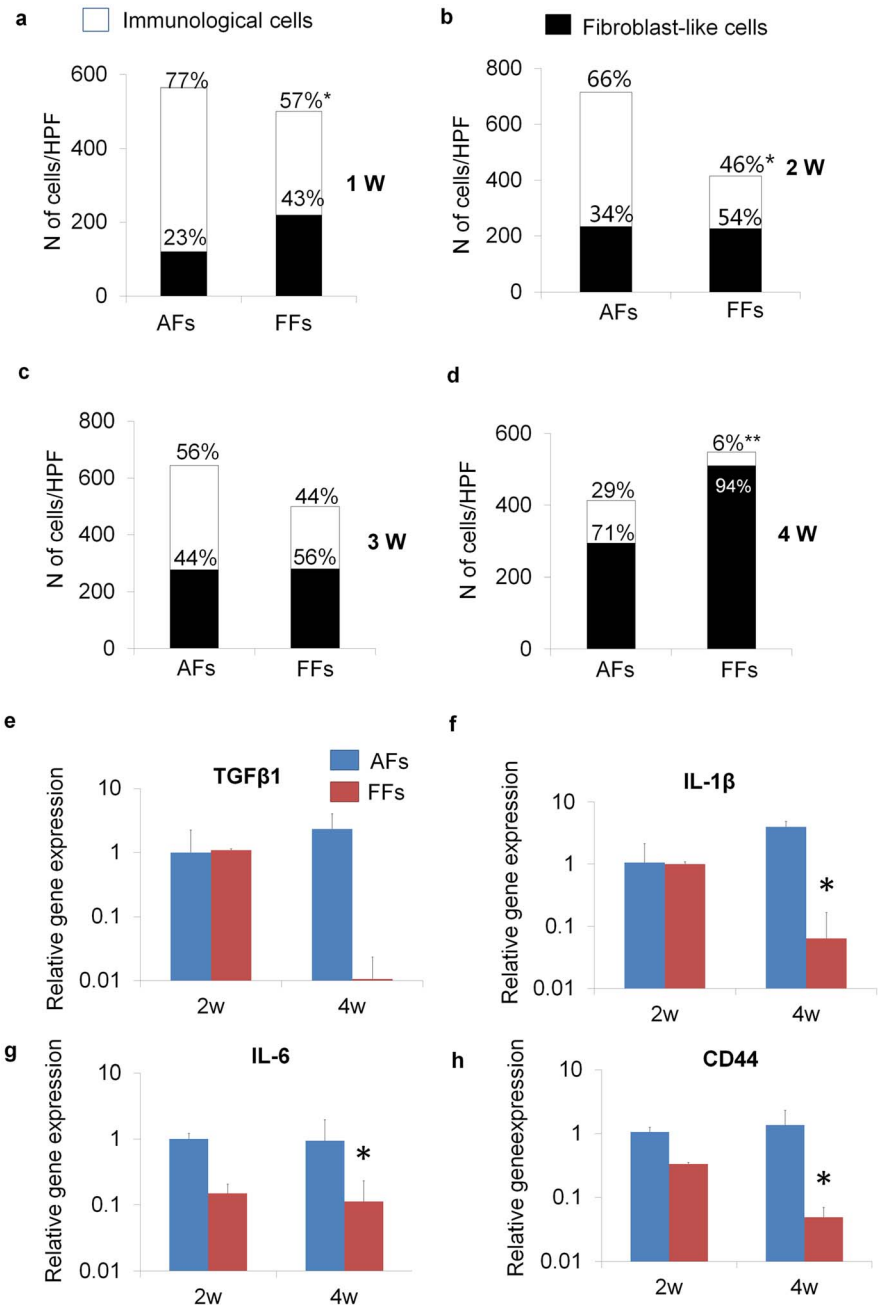

Figure 7 | The quantity and ratio of fibroblast-like cells and immune cells within the repaired tissue after 1 week (a), 2 weeks (b), 3 weeks (c) and 4 weeks (d) implantation. The FFs-repaired group had more fibroblast-like cells and less immune cells throughout the repair process compared to the AFs-repaired group. (e), (f), (g) and (h): mRNA levels of inflammatory cytokines within FFs and AFs at 2 weeks and 4 weeks post-implantation. Gene expression levels are normalized to the reference gene GAPDH (y axis), Transcript levels expressed relative to 2 w AF samples. The expression levels of inflammatory cytokines within FFs-repaired tendons were significantly down-regulated at 4 weeks post-surgery. HPF: high power field.* $p < 0.05$ between two groups. ** $p < 0.01$ between two groups.

fibroblast-like cells accounted for 44 ± 10.5% and immune cells accounted for 56 ± 10.5% (Fig. 7c). After 4 weeks post-surgery, the FFs-repaired group had more fibroblast-like cells (510 ± 96 vs. 294 ± 74/HPF, $p < 0.05$) and less immune cells (38 ± 47 vs. 118.8 ± 38/HPF, $p < 0.05$) compared to the AFs-repaired group (Fig. 7d). In the FFs treatment group, the repaired tissue was composed of approximately 94 ± 6.8% fibroblast-like cells, whereas in the AFs-repaired group, the repaired tissue was composed of only 71 ± 8.6% fibroblast-like cells (Fig. 7d; $p < 0.01$). This thus indicated that the injured tissues regenerated gradually over time.

Expression levels of cytokines involved in the inflammatory response, including TGF-beta1, CD44[25], IL-1beta and IL-6, were examined in the repaired tendons. TGFβ1 and CD44 expression in the FFs-repaired group at 4 weeks post-surgery was significantly down-regulated compared to at 2 weeks post-surgery, while expression of both TGFβ1 and CD44 were up-regulated in the AFs-repaired group. IL-1β expression was up-regulated during the repair process in the AFs-repaired group (Fig. 7f; $p < 0.05$) and down-regulated in the FFs group ($p < 0.05$). IL-6 displayed a similar expression profile, being significantly up-regulated at 4 weeks in the AFs group (Fig. 7g; 3.76-

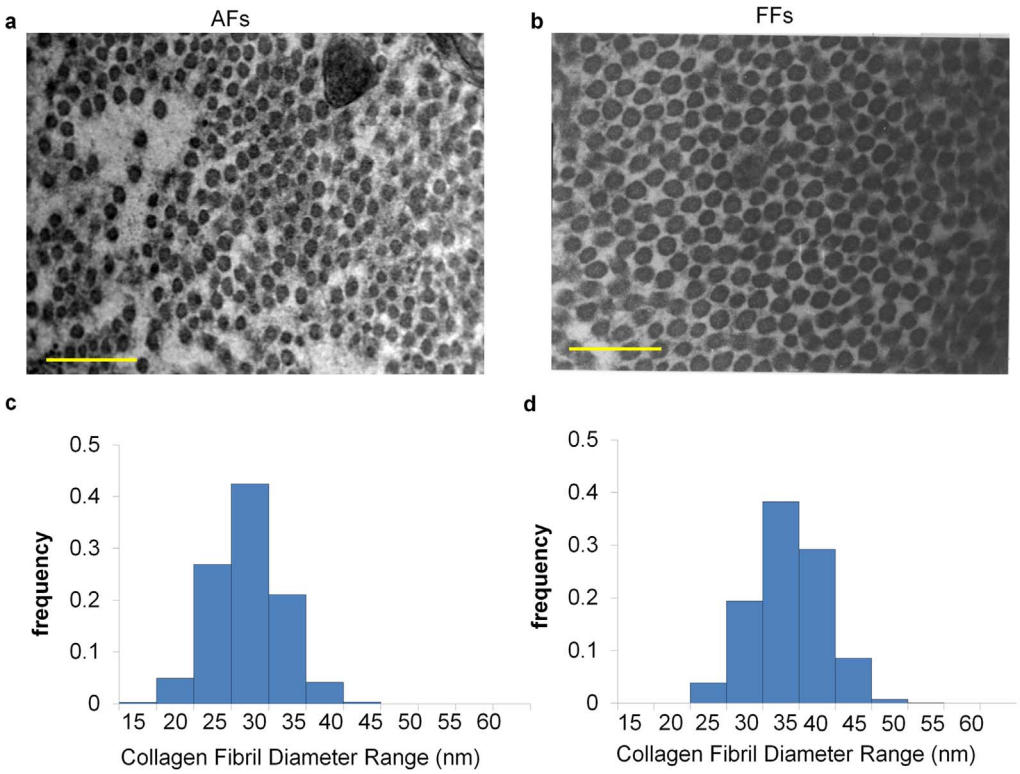

Figure 8 | Ultrastructure of tissue-engineered tendons at 4 weeks post-implantation. Histogram and distribution of collagen fibril diameters in the AFs group (a, c) and FFs group (b, d). There were thicker fibrils in the FFs-repaired group and larger diameter of collagen fibrils in the FFs-repaired tendons.

fold, $p < 0.05$) and down-regulated in the FFs group ($p < 0.05$) during the tendon repair process.

Ultrastructure of repaired tendons. To compare the distribution and diameter of collagen fibrils, specimens were observed under TEM. There were thicker fibrils in the FFs-repaired group compared to the AFs-repaired group (Fig. 8a and b). Although the collagen fibrils in the repaired tendons were still small and homogenous compared to normal tendons (Supplementary Figure c), the average diameter of collagen fibrils in the FFs-repaired tendons was (33.47 ± 0.59 nm, 2375 fibers), which was 21.9% larger than that of the AFs-repaired tendons (27.46 ± 1.78 nm, 1902 fibers, $p < 0.05$) (Fig. 8c and d).

Discussion

This study compared fetal cells and adult cells for Achilles tendon tissue engineering. The FFs group exhibited much better functional and structural properties with more collagen deposition, superior biomechanical properties and more physiological microstructure. In particular: (1) Scaffold-free engineered tendon can be utilized for functional tendon repair. (2) Fetal fibroblasts more readily formed tendon-like tissue. (3) Fetal cells significantly reduced infiltration of immune cells during the repair process, which enhanced tendon regeneration.

When mechanical testing was carried out at 4 weeks post-surgery, the FFs-repaired group yielded better results in the structural and functional properties of the regenerated tendons, as compared to the AFs-repaired group. The histological results demonstrated that the FFs-repaired tendons displayed more physiological ultrastructure, which correlated with the biomechanical properties. The FFs-repaired tendons had larger numbers of cells exhibiting spindle-shaped morphology, as well as exhibited relatively more parallel alignment compared to the AFs-repaired tendons. Consistent with the histology, continuous collagen fibers with bright yellow appearance was observed over the entire field of vision under polarized light microscopy, within the FFs-repaired tendons. These results thus indicated that FFs accelerated ECM deposition and remodeling, and also increased collagen deposition, compared to AFs.

More importantly, it was observed that there was formation of larger collagen fibrils within the FFs repaired group, thus indicating that FFs could improve the mechanical properties of the repaired tendon. Collagen is the major component of tendon ECM and collagen fibrils provide the major resistance to mechanical loading within connective tissues[42,43]. Previous studies have demonstrated that fibril diameter was heterogeneous within normal tendons, with all fibril size classes present, whereas repaired tendons are usually formed with scar tissue composed of small homogenous fibrils[43,44]. The increase in collagen fibril diameter is positively correlated with tendon biomechanical function[41,44,45]. Furthermore, FFs repaired tendons showed denser formation of collagen fibers (46.5 ± 5% vs. 32.1 ± 2.8%, $P < 0.05$) (Supplementary Figure d), which more closely resembled the native structure of tendon ECM. Although the average diameter of collagen fibril in the FFs-repaired tendon was still smaller than that of normal tendon tissue (77.01 ± 25.95 nm), the FFs-repaired tendons was 21.9% larger than that of the AFs-repaired tendons at 4 weeks post-implantation. Furthermore, under polarized light microscopy, unlike the AFs-repaired tendons, continuous collagen fibers (bright yellow) were observed over the entire field of vision in the FFs-repaired tendons. This indicated more mature collagen deposition in the FFs group. This was consistent with the better mechanical properties and histological morphology of the FFs-repaired tendons.

In our study, we found that fetal dermal fibroblasts are more likely to form engineered tendon in vitro, as confirmed by analysis of tendon-related gene expression and collagen deposition. Tenocytes are surrounded by an extensive extracellular matrix (ECM) composed predominantly of collagen[42]. Alterations in the ECM play an important role in cell adhesion, differentiation, and proliferation,

which may have profound effects on wound healing. Collagen I and collagen III are the most abundant ECM proteins of ligament and tendon tissue. A high expression level of collagen is required during tendon repair to reconstitute the extracellular matrix[46]. Therefore, higher expression of Col I and Col III during the early phase of cell sheet formation may indicate that FFs initiate transcription and translation earlier than AFs. The higher expression levels of tendon-related genes may contribute to better repair capacity of FFs in vivo upon transplantation. Biglycan (BGN), a member of the family of small leucine-rich proteoglycans (SLRP)[47,48], is highly expressed within connective tissues. BGN is considered to have an organizing role in ECM assembly.

The limitation of our study is that it is impossible to harvest autologous human fetal fibroblasts and difficult to obtain allogeneic fetal fibroblasts, which may impede the application of fetal cells. Although FFs treatment can enhance mouse Achilles tendon repair, the full regeneration process was still not achieved. Perhaps optimal regeneration requires a scaffold to form a cell-scaffold construct, which can also be incorporated with growth factors, cytokines and small molecule drugs[49]. Moreover, the mechanism involved in fetal tendon healing such as reduced inflammation has not yet been clearly elucidated. These need to be addressed in our future work.

The wound healing response in tendon involves inflammation and proliferation over several weeks[45,50]. Concurrent with the influx of inflammatory cells, the tendon regenerated from AFs displayed increased expression of TGF-β1, CD44, IL-1β and IL-6 at the injury site, whereas the tendon regenerated from FFs showed significantly lower expression of these genes. TGF-β1 is involved in tendon scar formation and is responsible for the recruitment and proliferation of fibroblasts and macrophages, up-regulation of metalloproteinase inhibitors, down-regulation of proteinase activity, and angiogenesis. Thus, it is associated with the formation of scar tissue following injury[25]. Scarless wounds in fetal mice have less TGF-β1 than neonatal or adult wounds[32,51]. CD44, together with its ligand hyaluronic acid are important mediators in healing and are over-expressed in fibrotic healing but under-expressed in scarless healing. CD44 has been implicated in multiple inflammatory events including leukocyte activation and adhesion, as well as pro-inflammatory cytokine release[25]. In a recent study, it was found that CD44 deficiency creates an environment that is conducive to regenerative healing, improving healing mechanics and increasing matrix and cytokine expression in a mouse patellar tendon injury model[52].

The difference in inflammatory response in adult and fetal wound healing plays a crucial role in tissue regeneration. An apparent complete lack of any such reaction or low expression levels of inflammatory factors in fetal tissues leads to regeneration of native tissue architecture[25]. Differences in recruitment of inflammatory cells to the injury site have important implications in tendon tissue engineering. This significant observation may aid in understanding the better regeneration capacity of FFs compared to AFs.

In conclusion, our study demonstrated that fetal cells might be more appropriate seed cells for tendon tissue engineering. Enhanced tendon regeneration was achieved using FFs as seed cells both in vitro and in vivo. As fetal cells play a key role in scarless regeneration, our results suggest that FFs initiate tendon regeneration by significantly reducing the inflammatory response at the injury site. These findings demonstrate that utilizing fetal fibroblasts may assist in the development of future strategies to treat tendon injuries.

Methods

Ethics statement. All studies were approved by the Zhejiang University Administration on Laboratory Animal Care. Animals were treated in accordance with IACUC guidelines (ethics approval number: ZJU2010101008).

Cell culture. FFs were isolated from mouse fetal dermis obtained from pregnant ICR mice between 10 & 12 days of gestation (E10-E12). The mice were purchased from animal centre of Zhejiang University. Briefly, the dermis of the fetuses was excised under sterile conditions and subjected to mincing, prior to incubation with 6 ml of 0.25% trypsin at 37°C for 20 min. Trypsin inactivation was achieved by addition of DMEM (Gibco-BRL Inc., Grand Island, NY, USA) supplemented with 10% (v/v) fetal bovine serum (FBS; Invitrogen, Carlsbad, CA, USA) and cells were then plated in 10 cm culture dishes and allowed to adhere for 24 h. AFs were isolated from the dorsal dermis of ICR mice (2 months). Excised skin pieces were digested with 2 ml of 0.2% collagenase solution (Gibco, Grand Island, NY) in DMEM (Gibco) for 24 hours. Non-adherent cells were subsequently discarded and cells in the adherent fraction were termed AFs. When the culture dishes became nearly confluent after about 14 days; the cells were detached and serially sub-cultured. Only cells at passage two (P2) were used in this study[53].

For the *in vitro* study, FFs and AFs were subjected to cell proliferation assay and gene expression analysis at different time points. Cell viability and proliferation were measured with a Cell Counting KIT-8 (CCK-8, Dojindo, www.dojindo.cn). Both the FFs and AFs, at desired time points, were incubated in CCK-8 solution in a 5% CO_2 incubator at 37°C for 3 h. The absorbance was measured at 450 nm with a reference wavelength of 650 nm. Cell number was correlated to optical density (OD)[54]. FFs and AFs were grown in 10 cm dishes until they reached 90% confluence, and the medium was subsequently supplemented with vitamin C[55] to encourage formation of cell sheet as engineered tendon. The cells were cultured in 12 pore plates for subsequent experiments. Therefore, the size of a sample is one pore plate. The cell sheets were harvested and subjected to H&E and Masson trichrome staining on day 14.

Cell labeling and detection. The cell sheets formed by FFs and AFs utilized for the *in vivo* study were pre-stained with DiI (1, 1′-dioctadecyl-3, 3, 3′3′-tetramethylindocarbocyanine perchlorate). Briefly, the cells were incubated with 5 ul/ml DiI (Sigma-Aldrich Inc., St. Louis, MO, USA) at 37°C for 20 min and then washed with PBS. After incubation in low glucose DMEM for another 20 min, the cells were observed under fluorescence microscopy (IX71; Olympus, Japan) at an excitation wavelength of 543 nm. After 2 and 4 weeks post-implantation, the animals were subjected to euthanasia, and the implanted tissues were harvested and histological sections were prepared. DAPI (Beyotime Institute of Biotechnology Inc., Jiangsu, China) was used to stain nuclei within the histological sections, and the positively-stained cells were observed under fluorescence microscopy. The count of survived cells was performed based on the pre-stained cells. The IPP 6.0 software was utilized for the cell counts. For each time point, there were four high power fields (HPF).

To evaluate the survival of implanted cells within the tendon defect, fluorescence imaging was carried out using a non-invasive Kodak *in vivo* FX small animal imaging system after 4 weeks post-implantation, as previously described[53]. A composite pseudo-color image representing light intensity (blue signifies least intense and red most intense) was obtained. The integrated light imaging was the result of 1 min exposure and acquisition. The specific excitation wavelength was at 550 nm, and the control excitation wavelength was at 470 nm to eliminate the background. The fluorescent image was superimposed in real time over the white light image of the tendon. The fluorescence intensity of the AFs-group ($n = 3$) and FFs-group ($n = 5$) was evaluated using the IPP 6.0 software at 2 weeks post-surgery.

Animal model. Fourteen female mice weighing 20–22 g were utilized. The AT was exposed through a lateral incision under general anesthesia. Then a gap wound was created and the Achilles tendon was removed to create a defect of 2 mm in length. On the left leg, the cell sheet composed of AFs (AFs were cultured and formed a cell sheet as scaffold-free engineered tendon) was sutured to the remaining AT using a non-resorbable suture (6-0 nylon) (AFs treated group, $n = 17$). On the right leg, a cell sheet composed of FFs was utilized to repair the defect (FFs treated group, $n = 17$). The wound was then irrigated and the skin was sutured. Post-surgery, the mice were allowed free cage activity at constant temperature with a 12-hour dark-light cycle and had unrestricted access to a standard diet and water. The sham procedure group refers to the non-injured tendon group. The sham-operated control group has received exactly the same surgical procedure as described above, ensuring that the scientific data reflect the effects of the experiment itself. A sham procedure group was used as a normal AT group in our study. The natural healing group was subjected to the same length tendon resection, but without any implant to promote healing.

At 1 week, 2 weeks, 3 weeks and 4 weeks post-implantation, the animals were sacrificed and two to three legs from each group were subjected to histological evaluation and gene expression analysis. For each sample, half was used for histology, the other half for RNA extraction. Seven legs were utilized for mechanical testing and then later for transmission electron microscopy (TEM) to assess the collagen fibril diameter at 4 weeks post-implantation. All animals were treated according to standard guidelines approved by the Zhejiang University Ethics Committee.

Histological assessment and Masson trichrome staining. The harvested specimens were immediately fixed in 10% (v/v) neutral buffered formalin, dehydrated through an alcohol gradient, cleaned, and then embedded in paraffin blocks. Histological sections (7 μm) were prepared using a microtome and subsequently subjected to hematoxylin and eosin staining (H&E). The quantity and ratio of fibroblast-like cells and immune cells within the repaired tissue was assessed, based on a modification of methods utilized in a previous study[56]. The histological sections were utilized for counts of fibroblast-like cells and immune cells. Briefly, the inflammatory cell count was based on the presence of macrophages, mast cells, neutrophils, and lymphocytes. The fibroblast-like cell count was based on the presence of spindle shaped cells and

collagen deposition. These cell counts were performed using the IPP 6.0 software. To avoid any bias in data collection, the selection and counting of cells were carried out by two experienced technicians. We selected and counted two high power fields (HPF) (n = 4–6 for each group), which was in the middle of the repaired tendon, for each sample of the repaired tendon at 1, 2, 3, and 4 weeks post-surgery. In addition, Masson trichrome staining was performed according to standard procedures to examine the general appearance of collagen deposition and collagen fibers[57].

Transmission electron microscopy (TEM). Tissue specimens were fixed by standard procedures[57] for TEM to assess collagen fibril diameter. Briefly, specimens were prefixed with 2% glutaraldehyde for 24 h and washed twice with PBS followed by post-fixation with 1% osmic acid for 2 h. After two washes in PBS, the specimens were dehydrated in an ethanol gradient and dried to a critical point. Then the specimens were mounted and sputter-coated with gold for viewing in a TEM (Quanta 10 FEI). About 500 collagen fibrils of each sample were measured to obtain a statistically accurate range of fibril diameter distribution.

Biomechanical evaluation. Mechanical testing was performed using an Instron tension/compression system with Fast-Track software (Model 5543 Instron, Canton, MA, USA)[53]. The hind limbs were wrapped in gauze soaked in saline and frozen at −20°C for later testing. Before testing, the hind limbs were gradually thawed to room temperature, and all soft tissue spanning the ankle, except for the center of the Achilles tendon, were sharply transected. Non-contact measurements of the tendon cross-sectional area were performed using two Vernier calipers. The triceps muscle-Achilles tendon-calcaneus complex (TACC) was then rigidly attached to custom-made clamps. The clamps secured the bone portion within its rectangular box compartment via a restraining pin. The lower clamp pinched the muscle tendon end, where a coarse-grade sandpaper interface was introduced to reduce the stress concentration as well as to prevent the tendon from slipping out of the clamp hold. The sandpaper interface introduced friction and provided the gripping system with a mechanism that allowed the grip on the tendon to be increased as more load is applied. This enabled the lower clamp to be adequately tightened without gripping the tendon to the point of significant damage[58]. Specimen orientation and alignment were maintained within the line of the applied tensile force. After applying a preload of 0.1 N, each TACC underwent pre-conditioning by cyclic elongation of between 0 and 0.5 mm for 20 cycles at 5 mm/min. This was followed by load to failure test at an elongation rate of 5 mm/min. The load–elongation behavior of the TACCs and failure modes were recorded. The structural properties of the TACC were represented by stiffness (N/mm), stress at failure (Mpa), modulus (Mpa) and maximum force (N). And the biomechanical values are compared to that of the sham procedure group. The non-resorbable suture (6-0 nylon) was rejected when the mechanical testing was performed. For each TACC, the greatest slope in the linear region of the load–elongation curve over a 0.5 mm elongation interval was used to calculate stiffness.

RNA isolation and RT-PCR. Total cellular RNA was isolated by cellular lysis in TRIZOL (Invitrogen Inc., Carlsbad, CA, USA) followed by a one-step phenol chloroform–isoamyl alcohol extraction, according to the manufacturer's instructions. The expression levels of various tendon-specific genes and inflammation-related genes in both the FFs and AFs groups were assessed by Q-PCR. This was achieved using Brilliant SYBR Green QPCR Master Mix (TakaRa) on a Light Cycler apparatus (ABI 7900HT) as previously described[54]. The primer sequences were designed using primer 5.0 software and are listed in Supplementary Tables 1 and 2. Each real-time PCR was performed on at least three different experimental samples, and the results are expressed as target gene expression normalized to GAPDH.

Statistical analysis. All data were compared using student's t test. Values of $p < 0.05$ were considered statistically significant.

1. Butler, D. L., Juncosa, N. & Dressler, M. R. Functional efficacy of tendon repair processes. *Annu Rev Biomed Eng* **6**, 303–29 (2004).
2. Bach, B. R. Jr. *et al.* Single-incision endoscopic anterior cruciate ligament reconstruction using patellar tendon autograft. Minimum two-year follow-up evaluation. *Am. J. Sports Med.* **26**, 30–40 (1998).
3. Bach, B. R. Jr. *et al.* Arthroscopically assisted anterior cruciate ligament reconstruction using patellar tendon autograft. Five- to nine-year follow-up evaluation. *Am. J. Sports Med.* **26**, 20–9 (1998).
4. Badylak, S. F. *et al.* The use of xenogeneic small intestinal submucosa as a biomaterial for Achilles tendon repair in a dog model. *J. Biomed. Mater. Res.* **29**, 977–85 (1995).
5. Maletius, W. & Gillquist, J. Long-term results of anterior cruciate ligament reconstruction with a Dacron prosthesis. The frequency of osteoarthritis after seven to eleven years. *Am. J. Sports Med.* **25**, 288–93 (1997).
6. Kew, S. J. *et al.* Regeneration and repair of tendon and ligament tissue using collagen fibre biomaterials. *Acta Biomater* **7**, 3237–47 (2011).
7. Ricchetti, E. T., Aurora, A., Iannotti, J. P. & Derwin, K. A. Scaffold devices for rotator cuff repair. *J. Shoulder Elbow Surg.* **21**, 251–65 (2012).
8. Longo, U. G., Lamberti, A., Maffulli, N. & Denaro, V. Tendon augmentation grafts: a systematic review. *Br. Med. Bull.* **94**, 165–88 (2010).
9. Shen, W. *et al.* Allogenous tendon stem/progenitor cells in silk scaffold for functional shoulder repair. *Cell Transplant.* **21**, 943–58 (2012).
10. Chen, X. *et al.* Force and scleraxis synergistically promote the commitment of human ES cells derived MSCs to tenocytes. *Sci Rep.* **2**, 977 (2012).
11. Yin, Z. *et al.* The effect of decellularized matrices on human tendon stem/progenitor cell differentiation and tendon repair. *Acta biomaterialia.* **9**, 9317–9329 (2013).
12. Ni, M. *et al.* Engineered scaffold-free tendon tissue produced by tendon-derived stem cells. *Biomaterials* **34**, 2024–37 (2013).
13. Dyment, N. A. *et al.* The Paratenon Contributes to Scleraxis-Expressing Cells during Patellar Tendon Healing. *PLoS One* **8**, e59944 (2013).
14. Barsby, T. & Guest, D. Transforming Growth Factor Beta3 Promotes Tendon Differentiation of Equine Embryo-derived Stem Cells. *Tissue Eng Part A.* **19**, 2156–64 (2013).
15. Guerquin, M. J. *et al.* Transcription factor EGR1 directs tendon differentiation and promotes tendon repair. *J. Clin. Invest.* **123**, 3564–76 (2013).
16. Schiele, N. R., Marturano, J. E. & Kuo, C. K. Mechanical factors in embryonic tendon development: potential cues for stem cell tenogenesis. *Curr. Opin. Biotechnol.* **24**, 834–840 (2013).
17. Cao, Y. *et al.* Bridging tendon defects using autologous tenocyte engineered tendon in a hen model. *Plast. Reconstr. Surg.* **110**, 1280–9 (2002).
18. Ouyang, H. W., Goh, J. C. & Lee, E. H. Use of bone marrow stromal cells for tendon graft-to-bone healing: histological and immunohistochemical studies in a rabbit model. *Am. J. Sports Med.* **32**, 321–7 (2004).
19. Krampera, M., Pizzolo, G., Aprili, G. & Franchini, M. Mesenchymal stem cells for bone, cartilage, tendon and skeletal muscle repair. *Bone* **39**, 678–83 (2006).
20. Connell, D., Datir, A., Alyas, F. & Curtis, M. Treatment of lateral epicondylitis using skin-derived tenocyte-like cells. *Br. J. Sports Med.* **43**, 293–8 (2009).
21. Liu, W. *et al.* Repair of tendon defect with dermal fibroblast engineered tendon in a porcine model. *Tissue Eng.* **12**, 775–88 (2006).
22. Deng, D. *et al.* Engineering human neo-tendon tissue in vitro with human dermal fibroblasts under static mechanical strain. *Biomaterials* **30**, 6724–30 (2009).
23. Clarke, A. W. *et al.* Skin-derived tenocyte-like cells for the treatment of patellar tendinopathy. *Am. J. Sports Med.* **39**, 614–23 (2011).
24. Beredjiklian, P. K. *et al.* Regenerative versus reparative healing in tendon: a study of biomechanical and histological properties in fetal sheep. *Ann. Biomed. Eng.* **31**, 1143–52 (2003).
25. Favata, M. *et al.* Regenerative properties of fetal sheep tendon are not adversely affected by transplantation into an adult environment. *J. Orthop. Res.* **24**, 2124–32 (2006).
26. Watts, A. E., Yeager, A. E., Kopyov, O. V. & Nixon, A. J. Fetal derived embryonic-like stem cells improve healing in a large animal flexor tendonitis model. *Stem Cell Res Ther* **2**, 4 (2011).
27. Rowlatt, U. Intrauterine wound healing in a 20 week human fetus. *Virchows Arch. A. Pathol. Anat. Histol.* **381**, 353–61 (1979).
28. Slate, R. K. *et al.* Fetal tibial bone healing in utero: the effects of miniplate fixation. *Plast. Reconstr. Surg.* **92**, 874–83 (1993).
29. Lin, K. Y., Posnick, J. C., al-Qattan, M. M., Vajsar, J. & Becker, L. E. Fetal nerve healing: an experimental study. *Plast. Reconstr. Surg.* **93**, 1323–33 (1994).
30. Coolen, N. A., Schouten, K. C., Middelkoop, E. & Ulrich, M. M. Comparison between human fetal and adult skin. *Arch. Dermatol. Res.* **302**, 47–55 (2010).
31. Lo, D. D., Zimmermann, A. S., Nauta, A., Longaker, M. T. & Lorenz, H. P. Scarless fetal skin wound healing update. *Birth Defects Res. C Embryo Today* **96**, 237–47 (2012).
32. Larson, B. J., Longaker, M. T. & Lorenz, H. P. Scarless fetal wound healing: a basic science review. *Plast. Reconstr. Surg.* **126**, 1172–80 (2010).
33. Brink, H. E., Stalling, S. S. & Nicoll, S. B. Influence of serum on adult and fetal dermal fibroblast migration, adhesion, and collagen expression. *In Vitro Cell. Dev. Biol. Anim.* **41**, 252–7 (2005).
34. Brink, H. E., Bernstein, J. & Nicoll, S. B. Fetal dermal fibroblasts exhibit enhanced growth and collagen production in two- and three-dimensional culture in comparison to adult fibroblasts. *J Tissue Eng Regen Med* **3**, 623–33 (2009).
35. Kishi, K., Okabe, K., Shimizu, R. & Kubota, Y. Fetal skin possesses the ability to regenerate completely: complete regeneration of skin. *Keio J. Med.* **61**, 101–8 (2012).
36. Longaker, M. T. *et al.* Adult skin wounds in the fetal environment heal with scar formation. *Ann. Surg.* **219**, 65–72 (1994).
37. Stalling, S. S. & Nicoll, S. B. Fetal ACL fibroblasts exhibit enhanced cellular properties compared with adults. *Clin. Orthop. Relat. Res.* **466**, 3130–7 (2008).
38. Lorenz, H. P. *et al.* Scarless wound repair: a human fetal skin model. *Development* **114**, 253–9 (1992).
39. Chen, J. L. *et al.* Efficacy of hESC-MSCs in knitted silk-collagen scaffold for tendon tissue engineering and their roles. *Biomaterials* **31**, 9438–51 (2010).
40. Shen, W. *et al.* The effect of incorporation of exogenous stromal cell-derived factor-1 alphawithin a knitted silk-collagen sponge scaffold on tendon regeneration. *Biomaterials* **31**, 7239–49 (2010).
41. Battaglia, T. C. *et al.* Ultrastructural determinants of murine achilles tendon strength during healing. *Connect. Tissue Res.* **44**, 218–24 (2003).
42. Waggett, A. D., Ralphs, J. R., Kwan, A. P., Woodnutt, D. & Benjamin, M. Characterization of collagens and proteoglycans at the insertion of the human Achilles tendon. *Matrix Biol.* **16**, 457–70 (1998).

43. Liden, M. *et al*. A histological and ultrastructural evaluation of the patellar tendon 10 years after reharvesting its central third. *Am. J. Sports Med.* **36**, 781–8 (2008).
44. Nakamura, N. *et al*. Decorin antisense gene therapy improves functional healing of early rabbit ligament scar with enhanced collagen fibrillogenesis in vivo. *J. Orthop. Res.* **18**, 517–23 (2000).
45. Lin, T. W., Cardenas, L. & Soslowsky, L. J. Biomechanics of tendon injury and repair. *J. Biomech.* **37**, 865–77 (2004).
46. Boykiw, R. *et al*. Altered levels of extracellular matrix molecule mRNA in healing rabbit ligaments. *Matrix Biol.* **17**, 371–8 (1998).
47. Iozzo, R. V. The biology of the small leucine-rich proteoglycans. Functional network of interactive proteins. *J. Biol. Chem.* **274**, 18843–6 (1999).
48. Zhang, G. *et al*. Development of tendon structure and function: regulation of collagen fibrillogenesis. *J Musculoskelet Neuronal Interact* **5**, 5–21 (2005).
49. Zhu, Y. & Li, M. [Research progress of cell-scaffold complex in tendon tissue engineering]. *Zhongguo Xiu Fu Chong Jian Wai Ke Za Zhi* **27**, 481–5 (2013).
50. Hoffmann, A. & Gross, G. Tendon and ligament engineering: from cell biology to in vivo application. *Regen Med* **1**, 563–74 (2006).
51. Nath, R. K., LaRegina, M., Markham, H., Ksander, G. A. & Weeks, P. M. The expression of transforming growth factor type beta in fetal and adult rabbit skin wounds. *J. Pediatr. Surg.* **29**, 416–21 (1994).
52. Ansorge, H. L., Beredjiklian, P. K. & Soslowsky, L. J. CD44 deficiency improves healing tendon mechanics and increases matrix and cytokine expression in a mouse patellar tendon injury model. *J. Orthop. Res.* **27**, 1386–91 (2009).
53. Chen, X. *et al*. Stepwise differentiation of human embryonic stem cells promotes tendon regeneration by secreting fetal tendon matrix and differentiation factors. *Stem Cells* **27**, 1276–87 (2009).
54. Yin, Z. *et al*. The regulation of tendon stem cell differentiation by the alignment of nanofibers. *Biomaterials* **31**, 2163–75 (2010).
55. Ouyang, H. W. *et al*. Mesenchymal stem cell sheets revitalize nonviable dense grafts: implications for repair of large-bone and tendon defects. *Transplantation* **82**, 170–4 (2006).
56. Shen, W. *et al*. The effect of incorporation of exogenous stromal cell-derived factor-1 alpha within a knitted silk-collagen sponge scaffold on tendon regeneration. *Biomaterials* **31**, 7239–49 (2010).
57. Woo, S. L., Takakura, Y., Liang, R., Jia, F. & Moon, D. K. Treatment with bioscaffold enhances the the fibril morphology and the collagen composition of healing medial collateral ligament in rabbits. *Tissue Eng.* **12**, 159–66 (2006).
58. Ouyang, H. W., Goh, J. C., Thambyah, A., Teoh, S. H. & Lee, E. H. Knitted poly-lactide-co-glycolide scaffold loaded with bone marrow stromal cells in repair and regeneration of rabbit Achilles tendon. *Tissue Eng.* **9**, 431–9 (2003).

Acknowledgments

This work was supported by NSFC grants (81330041,81125014, 31271041, 81201396,J1103603,81271970), Zhejiang Provincial Natural Science Foundation of China (LR14H060001). The National Key Scientific Program (2012CB966604), the National High Technology Research and Development Program of China (863 Program) (No.2012AA020503). Sponsored by Regenerative Medicine in Innovative Medical Subjects of Zhejiang Province and Zhejiang Provincial Program for the Cultivation of High-level Innovative Health talents. Medical and health science and technology plan of the department of Health of Zhejiang Province (2013RCA010,201341741).
No writing assistance was utilized in the production of this manuscript.

Author contributions

O.Y.H.W. and C.X. conceived and designed the experiments. T.Q.M. wrote the main manuscript text. S.W.L. and C.J.L., T.Q.M. performed the animal experiments. Y.Z. and T.Q.M. prepared figures 1–2. C.J.L. and T.Q.M. prepared figures 3–5. L.H.H. and F.Z., B.C.H. prepared figure 6. C.X. and S.W.L. prepared figures 7,8. All authors reviewed the manuscript.

Additional information

Supplementary information accompanies this paper at http://www.nature.com/scientificreports

Competing financial interests: The authors declare no competing financial interests.

How to cite this article: Tang, Q.-M. *et al*. Fetal and adult fibroblasts display intrinsic differences in tendon tissue engineering and regeneration. *Sci. Rep.* **4**, 5515; DOI:10.1038/srep05515 (2014).